RESEARCH ARTICLE

Global Ecology and Biogeography | A Journal of Macroecology

WILEY

The distribution of global tidal marshes from Earth observation data

Thomas A. Worthington[1] [ORCID] | Mark Spalding[1,2] | Emily Landis[3] | Tania L. Maxwell[1,4] |
Alejandro Navarro[5] | Lindsey S. Smart[3] | Nicholas J. Murray[5]

[1]Conservation Science Group, Department of Zoology, University of Cambridge, Cambridge, UK

[2]The Nature Conservancy, Department of Physical, Earth, and Environmental Sciences, University of Siena, Siena, Italy

[3]Ocean and Climate Team, The Nature Conservancy, Arlington, Virginia, USA

[4]Biodiversity, Ecology and Conservation Research Group, International Institute for Applied Systems Analysis (IIASA), Laxenburg, Austria

[5]College of Science and Engineering, James Cook University, Townsville, Queensland, Australia

Correspondence
Thomas A. Worthington, Conservation Science Group, Department of Zoology, University of Cambridge, Cambridge CB2 3QZ, UK.
Email: taw52@cam.ac.uk

Abstract

Aim: Tidal marsh ecosystems are heavily impacted by human activities, highlighting a pressing need to address gaps in our knowledge of their distribution. To better understand the global distribution and changes in tidal marsh extent, and identify opportunities for their conservation and restoration, it is critical to develop a spatial knowledge base of their global occurrence. Here, we develop a globally consistent tidal marsh distribution map for the year 2020 at 10-m resolution.

Location: Global.

Time period: 2020.

Major taxa studied: Tidal marshes.

Methods: To map the location of the world's tidal marshes at 10-m resolution, we applied a random forest classification model to Earth observation data from the year 2020. We trained the classification model with a reference dataset developed to support distribution mapping of coastal ecosystems, and predicted the spatial distribution of tidal marshes between 60°N and 60°S. We validated the tidal marsh map using standard accuracy assessment methods, with our final map having an overall accuracy score of 0.85.

Results: We estimate the global extent of tidal marshes in 2020 to be 52,880 km^2 (95% CI: 32,030 to 59,780 km^2) distributed across 120 countries and territories. Tidal marsh distribution is centred in temperate and Arctic regions, with nearly half of the global extent of tidal marshes occurring in the temperate Northern Atlantic (45%) region. At the national scale, over a third of the global extent (18,510 km^2; CI: 11,200–20,900) occurs within the USA.

Main conclusions: Our analysis provides the most detailed spatial data on global tidal marsh distribution to date and shows that tidal marshes occur in more countries and across a greater proportion of the world's coastline than previous mapping studies. Our map fills a major knowledge gap regarding the distribution of the world's coastal ecosystems and provides the baseline needed for measuring changes in tidal marsh extent and estimating their value in terms of ecosystem services.

1 | INTRODUCTION

Tidal marsh ecosystems are vegetated coastal wetlands located in areas of regular to occasional tidal inundation, formed by a broad variety of herbaceous and woody vascular plants (Adam, 2002). Whilst dominated by saline and brackish marshes, they include areas of freshwater tidal marsh (Barendregt, 2018; Mitsch & Gosselink, 2015). They occur along many of the world's sheltered, sediment-dominated coastlines, particularly in temperate and arctic regions (Tiner & Milton, 2018). They are also an important, yet frequently overlooked, coastal ecosystem in many arid and tropical regions (Viswanathan et al., 2020). Tidal marsh vegetation occurs between mean high water neaps up to the limits of the highest astronomical tide (Adam, 2002), often with distinct zonation across the tidal frame (Mitsch & Gosselink, 2015; Scott et al., 2014a, 2014b; Tiner & Milton, 2018). Tidal marshes show close ecological and physical linkages with adjacent coastal ecosystems, including unvegetated intertidal flats, shellfish beds and reefs and seagrass beds lower in the tidal frame (Adam, 2002). The term salt marsh is also widely used and broadly overlaps with tidal marsh; however, the former may include non-tidal and inland marshes, while tidal marshes, in some places can be freshwater systems. Tidal marshes often form part of mosaicked environments together with mangroves or salt pans, particularly in warm temperate to tropical regions (Lopez-Portillo & Ezcurra, 1989; Rodriguez et al., 2016).

Tidal marshes are subject to a multitude of anthropogenic pressures, primarily because they are often located close to the most densely populated coastal areas of the planet (Neumann et al., 2015). Their loss and degradation have been caused by a range of factors, tracing back over centuries and even millennia (Airoldi & Beck, 2007; Allen, 2000). These include land reclamation for conversion to agriculture and coastal infrastructure (Davy et al., 2009; Gedan & Silliman, 2009; Gu et al., 2018; Melville et al., 2016; Shi-lun & Ji-yu, 1995), aquaculture and salt production (Almeida et al., 2014) and invasion of _Spartina alterniflora_ outside its native range (Zheng et al., 2018). In addition, tidal marshes are likely to be impacted by the multifaceted threats linked to climate change, including sea level rise and associated coastal squeeze, increased magnitude and frequency of extreme weather events and changes in precipitation and temperature (Adams, 2020; Silliman et al., 2005). The evidence of climate change impacts has already been detected with the reduction in extreme cold events allowing the poleward expansion of mangroves into tidal marsh habitat (Cavanaugh et al., 2014, 2019).

Recently, tidal marshes, alongside other coastal wetlands such as mangroves and seagrass, have garnered significant attention for their conservation value and restoration potential. In addition to their significance for biodiversity, tidal marshes have been recognized as supporting multiple ecosystem services, including carbon sequestration (Friess et al., 2020; zu Ermgassen et al., 2021). Tidal marshes are highly productive, with sequestration rates greater than some other terrestrial ecosystems (on average, 210g CO_2 $m^{-2}yr^{-1}$) (Chmura et al., 2003; Hopkinson et al., 2012), with potential global carbon stocks in the top metre of tidal marsh soil estimated at 1.22 ± 0.20 Pg C (Maxwell et al., 2023). Tidal marsh vegetation also helps attenuate wave energy (Möller et al., 2014), therefore, providing storm protection benefits to coastal communities (Costanza et al., 2008; Shepard et al., 2011). For example, wetlands are estimated to have avoided $625 Million in property damage during Hurricane Sandy (Narayan et al., 2017). They are important areas for tourism and recreation (Barbier et al., 2011) and they help support healthy fisheries that provide food and income for millions of people (Baker et al., 2020; Jänes et al., 2020). However, our ability to comprehensively estimate the value of tidal marshes and develop coordinated strategies for their protection and restoration at large scales is hindered by limited knowledge of their global distribution.

Tidal marshes can be identified from satellite images (Tiner & Milton, 2018); however, unlike other coastal ecosystems such as coral reefs (Li et al., 2020), mangroves (Bunting et al., 2022; Giri et al., 2011) and tidal flats (Murray et al., 2019), spatial mapping of tidal marshes has generally been conducted at local or regional scales. Until now, there has been no globally consistent map of tidal marshes, and their total extent has been poorly quantified as a result (McLeod et al., 2011; Pendleton et al., 2012).

Efforts to map tidal marshes have utilized different methods, across different time periods, making comparisons across time and space unreliable. Where larger scale assessments exist, they tend to focus on well-studied regions such as the U.S.A. (U.S. Fish and Wildlife Service, 2021), China (Hu et al., 2021), Australia and parts of South America (Isacch et al., 2006). The most recent global assessment of tidal marsh spatial distribution collated Geographic Information System (GIS) data from peer-reviewed articles and grey literature, including spatial data from government agencies, non-governmental organizations and research institutions (Mcowen et al., 2017). In total, the authors identified almost 55,000 km^2 of tidal marshes across 43 countries and territories, although they also identified several large regions—Canada, Northern Russia, South America and Africa—for which data were lacking (Mcowen et al., 2017). In a global assessment of all wetlands, Zhang et al. (2023) also included a category of tidal salt marsh, mapping approximately 75,000 km^2, with other estimates from the literature ranging from 22,000 to 400,000 km^2 (McLeod et al., 2011; Pendleton et al., 2012). Other efforts to characterize tidal marsh dynamics globally have typically focused on change analyses (Campbell et al., 2022; Murray, Worthington, et al., 2022) or simulation (Schuerch et al., 2018); however, a consistent medium-resolution map baseline has yet to be established.

Here, we create a globally consistent tidal marsh distribution map for the year 2020 at 10-m resolution. To do this, we leverage the extensive archive of analysis-ready, publicly available remote-sensing imagery, combining optical and radar images from the European Space Agency's Sentinel missions (Berger et al., 2012). This is coupled with an open-access global repository of global training and validation data (Murray, Bunting, et al., 2022). This wealth of data was analysed using the high-performance processing capabilities of the Google Earth Engine platform, which supports rapid planetary-scale remote-sensing data analyses (Gorelick et al., 2017). The tidal marsh distribution dataset provides a critical baseline for future analyses of changes in tidal marsh distribution and condition, and valuation of tidal marsh ecosystem services.

2 | MATERIALS AND METHODS

To map the distribution of the world's tidal marshes facilitating more accurate estimates of extent and underpinning future analyses of tidal marsh change, we developed a supervised classification of globally comprehensive Earth observation data (Supporting Information Figure S1). We used 10-m resolution active (Sentinel 1) and passive (Sentinel 2) data acquired in 2020 (Berger et al., 2012) and an open access reference dataset (Murray, Bunting, et al., 2022) to parameterize a random forest classification model that enabled the prediction of tidal marsh occurrence over the study area.

2.1 | Covariate data

To develop a covariate set suitable to support the classification model, we filtered all images in the Sentinel 1 and 2 archives for the year 2020, retaining all images within our mapping area. The mapped area was confined between 60°N and 60°S, and within a coastal zone data mask (after Murray, Worthington, et al., 2022). In total, 287,320 optical and 143,067 radar images were processed.

Sentinel 2 Level 2 data from the Google Earth Engine Data Catalogue were used and represent atmospherically corrected surface reflectance processed using sen2cor (Main-Korn et al., 2017). Sentinel 2 imagery contains 12 spectral bands, with pixel resolutions between 10 and 60 m, and band data values ranging from 0 to 1 (albeit with a scale factor of 0.0001 in Google Earth Engine). Global scale remote sensing necessitates automated methods for addressing known sources of map commission and omission error. As a prime source of these errors and to promote computational efficiency, we opted to remove images where metadata indicated a high proportion of cloudy pixels (≥20%). Further masks were applied to remove pixels flagged in image metadata as clouds, cloud shadow or snow. Three spectral indices that represent either vegetation or water dynamics, and are, therefore, useful to discriminate tidal marshes from other land classes in a classification model, were calculated for every image. The normalized difference vegetation index

(NDVI) is the normalized ratio of the near-infrared (NIR) band which is reflected by vegetation and the red band which is absorbed by vegetation (Pettorelli et al., 2005).

$$NDVI = \frac{(NIR - Red)}{(NIR + Red)} \tag{1}$$

Values range between −1 and +1, with values closer to +1 representing areas of dense green vegetation. The enhanced vegetation index (EVI) was developed to reduce the influence of atmospheric conditions and decouple the canopy background signal (Huete et al., 2002). In addition to the NIR and red bands used in NDVI, EVI uses the blue band to reduce the impact of atmospheric effects (Schultz et al., 2016).

$$EVI = G \times \frac{(NIR - Red)}{(NIR + C_1 \times Red - C_2 \times Blue + L)} \tag{2}$$

The coefficient L is the canopy background adjustment and C_1 and C_2 are used with the blue band to reduce aerosol influences on the red band (Huete et al., 2002). Values of $L=1$, $C_1=6$, $C_2=7.5$ and $G=2.5$ were used (Huete et al., 2002). The automated water extraction index (AWEI) combines the green, NIR and short-wave infrared (SWIR) bands to identify areas of water (Feyisa et al., 2014).

$$AWEI = 4 * \frac{(Green - SWIR)}{(0.25 * NIR + 2.75 * SWIR)} \tag{3}$$

An annual composite of the optical images was created by taking the median, the 10th, 25th, 75th and 90th percentiles, the standard deviation and the 5th–95th, 10th–90th and 25th–75th interval means of the NDVI, EVI and AWEI spectral indices and the raw NIR band, resulting in an initial set of 36 covariates. Composite indices were developed from five of the 12 bands of the Sentinel 2 data. Annual composite indices were used to reduce the impact of clouds, cloud shadow or snow on the indices, as they represent complex spectral dynamics in a manner suitable for a pixel-based classification model, and have been shown to be effective in estimating the distribution of a range of other coastal ecosystem types (Murray et al., 2019; Murray, Worthington, et al., 2022). These indices were used to discriminate between vegetated areas (NDVI, EVI) and water (AWEI), while the NIR band has been used extensively to identify mangroves (Kuenzer et al., 2011), a closely associated coastal ecosystem.

Exploratory analysis of 41,138 training points annotated with data values from the 36 predictors revealed high collinearity between the covariates derived from the optical data. A priori we retained the median and standard deviation covariates, and used the *findCorrelation* function from the 'caret' R package (Kuhn, 2021) in R to remove highly correlated covariates from the remaining 28 covariates. Based on a threshold of $r<0.9$, we removed 17 highly correlated covariates from the covariate set, resulting in a final set of 19 covariates for the classification model (Supporting Information Table S1). While the inclusion of highly correlated predictor variables can impact the identification of variables of importance within machine learning models (Nicodemus & Malley, 2009), as the focus of

this analysis was developing the most accurate tidal marsh map, we allowed a less stringent correlation coefficient threshold than has been previously advocated (e.g. Dormann et al., 2013).

Each Sentinel 1 scene in Google Earth Engine is pre-processed using the Sentinel-1 Toolbox (Veci et al., 2014). This pre-processing consists of the following steps: removal of discontinuities between sub-swaths for scenes in multi-swath acquisition mode using thermal noise removal, application of radiometric calibration values and application of terrain correction in high latitudes using the SRTM or ASTER DEMs. The Sentinel 1 radar data were filtered to those images with VV and VH polarizations, and indices that represented the span and total of the scattering power, the difference between co- and cross-polarized observations and the ratio of the VV and VH polarizations (Mahdianpari et al., 2019), were calculated for each image. An annual composite of the radar images was created by taking the median of the raw VV and VH polarizations and the span, difference and ratio indices, resulting in five covariates (Supporting Information Table S1).

$$\text{Span} = |S_{VV}|^2 + |S_{VH}|^2 \tag{4}$$

$$\text{Difference} = |S_{VV}|^2 - |S_{VH}|^2 \tag{5}$$

$$\text{Ratio} = \frac{|S_{VV}|^2}{|S_{VH}|^2} \tag{6}$$

In addition to the radar and optical data, three covariates were included to assist in differentiating tidal marshes from other land classes that occur in coastal environments. Firstly, a global map of the probability of occurrence of tidal wetlands derived from over 1.1 million satellite images acquired by Landsat 5 to 8 (Murray, Worthington, et al., 2022) was used to inform the potential distribution of tidal marsh ecosystems. A global elevation model that combines land topography and ocean bathymetry (Amante & Eakins, 2009) was used to inform the classification model about real features of coastal environments that influence the distribution of tidal marshes, while an annual composite of monthly nightlight data from the year 2020 (Elvidge et al., 2017) was included to assist differentiation of urban and industrial areas.

The optical and radar data and the three additional covariates (Supporting Information Table S1) were combined into a single composite image. Within Google Earth Engine, superpixel clustering based on the Simple Non-Iterative Clustering image segmentation algorithm was then applied to the composite image (Achanta & Süsstrunk, 2017). The image segmentation clusters areas of homogenous pixels and helps to reduce false positives in terms of individual pixels of the prediction class being predicted across the image. The pixel values for each band within a cluster are converted into the mean value of the band across the cluster, and as such the prediction of each pixel within a cluster results in the same classification. Such object-based approaches have been shown to have a superior predictive power to pixel-based classification when mapping coastal environments (Lyons et al., 2020; Mahdianpari et al., 2019).

2.2 | Training data

To parametrize the random forest classification model, we collated a training dataset consisting of the known locations of five classes: tidal wetland ecosystems (tidal marshes, mangroves and tidal flats) and non-tidal wetland types (permanent water and other terrestrial areas). The training set was assembled from three sources. Firstly, 136,404 points from the *coastTrain* dataset (Murray, Bunting, et al., 2022), which was created to provide reference data for coastal ecosystem remote-sensing classification models. Secondly, a further 8789 points were developed to map coastal ecosystems in Australia (A. Navarro, personal communication). Finally, 754 tidal marsh locations were collected specifically for this analysis. The 754 tidal marsh points were targeted at regions that had reduced coverage in the coastTrain dataset, such as South Africa, East Asia (outside China), the Middle East and the Pacific coast of South America. Potential locations of tidal marshes in these regions were identified from published literature and online sources. Visual interpretation of high-resolution satellite images available from Google Earth, alongside NIR and false colour composites from Landsat imagery were used to select pixels that represented tidal marshes. The combined training dataset consisted of a high number of mangrove locations from the coastTrain dataset; therefore, a random sample of only 10,000 of the mangrove points was used to balance the training data. This resulted in a final training dataset of 41,762 points, including 9811 tidal marsh locations (Supporting Information Figure S2).

2.3 | Tidal marsh distribution model

To map the global distribution of tidal marshes, we developed a random forest classification model. Machine learning approaches such as random forest have been applied to a variety of ecological and remote-sensing topics due to their high classification accuracy and ability to rapidly model large datasets with complex interactions between predictor variables (Belgiu & Drăgu, 2016; Cutler et al., 2007). Machine learning approaches have been effectively applied to mapping coastal ecosystems such as intertidal wetlands (Murray, Worthington, et al., 2022), tidal flats (Murray et al., 2019), mangroves (Bunting et al., 2018) and coral reefs (Lyons et al., 2020). Future application of more complex deep learning or neural network models, or classifiers such as XGBoost which have been shown to be effective at detecting coastal vegetated ecosystems (Fu et al., 2022) may further increase prediction accuracy.

2.3.1 | Model tuning

The training data were combined into two classes, tidal marshes and non-tidal marshes (permanent water, other terrestrial areas, mangroves and tidal flats). Before parametrizing the model in Google Earth Engine, we firstly tuned the random forest hyper-parameters using iterative testing of a hypergrid of potential values. Models

WORTHINGTON ET AL.

Global Ecology
and Biogeography

A Journal of
Macroecology

WILEY

5 of 13

were fitted using the training data and R package 'ranger' (Wright & Ziegler, 2017). The hypergrid consisted of 375 potential model parameterizations with differing values for the number of trees grown, the number of covariates sampled at each split, the fraction of observations sampled at each split and the minimum node size. To account for minimal differences in the model fits (based on out-of-bag error rate) between the best fitting parametrizations, the median of the top 10 models based on the hypergrid search was used in Google Earth Engine.

An initial model was fitted to the training data in Google Earth Engine with a random 80:20% training: validation split. Exploratory analysis suggested high overall accuracy (96.4%) on the validation dataset, with a Kappa coefficient of 0.90, and an omission error for the different classes of 0.02 non-tidal marsh, 0.09 tidal marsh and a commission error for the different classes of 0.03 non-tidal marsh, 0.06 tidal marsh. Owing to this high initial model accuracy, a final random forest classification model was then fitted in Google Earth Engine using all the training data. The final random forest classification model was then applied to the segmented composite image (containing the optical, radar and three additional covariates, Supporting Information Table S1), and each pixel was classified as either tidal marsh or not.

2.3.2 | Post-processing

The initial predicted distribution of tidal marshes was then refined using a post-processing procedure consisting of several steps. Areas that were predicted to have a low probability (<50%) of being a coastal wetland based on the work of Murray, Worthington et al. (2022) were removed, as were areas greater than 10m in elevation using the MERIT Digital Elevation Model (Yamazaki et al., 2017) and those areas that overlapped with the predicted 2020 mangrove distribution (Bunting et al., 2022). The minimum mapping unit of the global tidal marsh map was tested for two areas (1 ha vs. 10 ha) by identifying areas that had a minimum of either 100 or 1000 connected pixels.

2.3.3 | Validation

This post-processed model prediction was validated using 2300 randomly sampled points developed using the following stratified sampling procedure. Points were sampled equally across 10 of the 11 biogeographical realms in the Marine Ecoregions of the World (Spalding et al., 2007). One hundred points were sampled from the non-tidal marsh class, as were a further 100 points classified as tidal marsh in both the 1-hectare and 10-hectare minimum mapping unit map versions. Finally, an additional 30 points classified as tidal marsh only in the 1-hectare minimum mapping unit version were sampled. A single image analyst used Google Satellite, Bing Maps and Google Earth Pro imagery to assess each point of the validation set and assign it to one of three groups, 'tidal marsh', 'other' or 'unknown' using the Class Accuracy plugin in QGIS (Bunting, 2020). The model prediction for the point was concealed from the reviewer during the validation process. The 'unknown' assignment in the validation set was used for points where no confident assignment of the ecosystem type was possible, primarily due to poor reference imagery or a lack of information available about tidal marshes in particular regions, predominantly in parts of the tropics.

Accuracy statistics were calculated for the different realms using the 'caret' R package (Kuhn, 2021) in R (R Core Team, 2023). Only validation points assigned to the groups 'tidal marsh' and 'other' were used to calculate the accuracy statistics ($n = 1708$). For overall and commission errors, the validation statistics for the vast majority of realms were higher for the 10-hectare minimum mapping unit version (Supporting Information Table S2) in comparison to the 1-hectare minimum mapping unit version (Supporting Information Table S3), and this was, therefore, the version used for the final mapping product. Accuracy was very variable across the realms, with temperate regions generally achieving higher overall map accuracy. The commission errors were always higher than the omission errors, which in the tropics was very high. To address the issues identified during the map validation, we undertook two final post-processing procedures. We removed areas of tidal marsh that had been identified as aquaculture ponds in 10 countries in Asia, following Murray, Worthington, et al. (2022), and manually corrected misclassifications. Manual correction was carried out by visually assessing the map outputs and removing obvious misclassifications. Misclassifications were generally related to areas of aquaculture and flooded agriculture such as rice fields and rocky shorelines.

The 1708 previously classified validation points were then compared to the final version of the map, and accuracy statistics were again calculated. The manual corrections greatly improved the overall accuracy across the realms, with the largest improvements in tropical regions, although commission errors remained much greater in those regions (Table 1). We used resampling procedures to calculate the confidence intervals around our global accuracy statistics (Lyons et al., 2018), which were used to propagate uncertainty around derived estimates of global and regional tidal marsh extent. We resampled ($n = 1000$ iterations) the validation points using the mean of the samples as our estimates of accuracy, and the 0.025 and 0.975 percentiles to create the 95% confidence intervals (Supporting Information Table S4). Our final map had an overall accuracy of 0.85 (95% confidence interval (CI): 0.84–0.87). The resampling procedure allowed for asymmetry in the confidence intervals around our tidal marsh extent estimates, which better represent the unevenness in the omission and commission errors identified in our map (Supporting Information Tables S4 and S5). We used the 0.05 percentile of the commission and omission error estimates from the

Realm	Overall accuracy	Kappa	Omission error	Commission error	N
Temperate Northern Atlantic	0.88	0.76	0.05	0.20	200
Temperate Northern Pacific	0.81	0.60	0.12	0.36	171
Tropical Atlantic	0.80	0.38	0.20	0.66	129
Western Indo-Pacific	0.73	0.13	0.29	0.89	151
Central Indo-Pacific	0.91	0.69	0.23	0.27	171
Eastern Indo-Pacific	0.93	0.43	0.14	0.68	190
Tropical Eastern Pacific	0.85	0.09	0.00	0.94	114
Temperate South America	0.80	0.59	0.10	0.37	188
Temperate Southern Africa	0.89	0.78	0.11	0.16	197
Temperate Australasia	0.88	0.75	0.08	0.18	197

Note: Omission and commission error statistics given for tidal marsh class only. The number of sample points (*N*) within each realm is the maximum number assessed (*n* = 200) minus those classified as unknown during the validation assessment.

resampled distribution to calculate the upper and lower bounds of all area estimates using the formulas:

$$\text{area}_{TM}\text{lower} = \text{area}_{TM} - (\text{area}_{TM} * \text{commission}_5)$$

$$\text{area}_{TM}\text{upper} = \text{area}_{TM} + (\text{area}_{TM} * \text{omission}_5)$$

where area_{TM} is the area of tidal marsh, commission_5 and omission_5 are the 0.05 percentile of the commission and omission error estimates respectively.

2.3.4 | Extent statistics

Tidal marsh area was summarized at the marine ecoregion realm level (Spalding et al., 2007) and for countries and territories using the union of the ESRI world country database and the Exclusive Economic Zones version 11 (Flanders Marine Institute, 2020). The percentage of the tidal marsh contained within protected areas in each country was calculated using The World Database on Protected Areas (WDPA; UNEP-WCMC and IUCN, 2023). The WDPA was cleaned following standard procedures (Hanson, 2022), which included removing polygon vertices, removing protected areas where the status was proposed or unknown and dissolving protected area polygons to prevent double counting of overlapping protected areas.

3 | RESULTS AND DISCUSSION

Knowledge of the distribution of tidal marsh ecosystems is essential to understand fundamental drivers of their dynamics, estimate risks to their persistence, establish baselines for assessing a range of national-to-global conservation targets and to provide a basis for accounting for their ecosystem service provisioning. Our study reports the development of the first global, 10-m resolution thematic map of tidal marsh distribution, and allows a range of analyses that can fill these important knowledge gaps.

3.1 | Global and regional estimates

We estimate the global extent of tidal marshes in 2020 to be 52,880 km² (CI: 32,020 to 59,780 km²). This estimate is lower than many earlier estimates generated by diverse mapping approaches and confirms that tidal marshes occupy a considerably smaller area than other coastal ecosystems such as, for example, mangroves 147,359 km² (Bunting et al., 2022) and tidal flats 127,921 km² (Murray et al., 2019).

Table 2 shows the estimates of tidal marsh extent by biogeographic realm (Spalding et al., 2007). The findings highlight the predominance of these ecosystems in the temperate and Arctic realms, and the particular importance of the temperate Northern Atlantic. This single realm hosts 45% of the world's tidal marshes, with extensive areas along the Atlantic and Gulf of Mexico coasts of the U.S.A and in the Northern European Seas province (Figure 1). The widespread distribution of marshes in this region is likely to be a product of multiple geological and geomorphological factors influencing the abundance of extensive, protected and low-elevation coastal sediments. Climate too is important—it is too cold for mangroves, but not influenced by ice scour. (Scott et al., 2014a). As noted by previous authors, this realm is also the centre of floristic diversity for tidal marshes (Adam, 1990; Chapman, 1974). We estimate that the temperate Northern Pacific Realm also has significant areas of tidal marshes, especially around the coasts of southern Alaska and the Russian coasts of the Sea of Okhotsk, an area that was unmapped by Mcowen et al. (2017).

The area of tidal marshes in the southern hemisphere is 8380 km² (CI: 5080 to 9480 km²) representing only 16% of the full extent of coastal tidal marsh we detected in our analysis. However, the Atlantic coast of South America in particular supports extensive tidal marshes on estuaries with large discharges (Hatje et al., 2023). Isacch et al. (2006) estimated some 2133 km² of tidal marshes in the area between southern Brazil and central Argentina, which is lower than our estimate of 3060 km² for that region. Our prediction for Temperate Southern Africa confirms prior observations that these are indeed scarce habitats in this realm (Adams, 2020).

TABLE 2 The extent of tidal marshes by biogeographic realm (Spalding et al., 2007).

Realm	Area (km^2)	95% confidence interval	% of global Total
Arctic[a]	9210	5580–10,410	17.4
Central Indo-Pacific	600	360–670	1.1
Eastern Indo-Pacific	<10	–	<0.01
Southern Ocean	–	–	–
Temperate Australasia	2040	1230–2300	3.9
Temperate Northern Atlantic	23,760	14,390–26,860	44.9
Temperate Northern Pacific	6580	3980–7440	12.4
Temperate South America	3790	2300–4290	7.2
Temperate Southern Africa	80	50–100	0.2
Tropical Atlantic	4810	2920–5440	9.1
Tropical Eastern Pacific	80	50–90	0.2
Western Indo-Pacific	1920	1170–2180	3.6
Total	52,880	32,020–59,780	

Note: 95% confidence intervals created by resampling ($n = 1000$) the validation points and using the 0.05 percentile of the commission and omission error estimates.

[a]N.B. our map does not extend beyond 60°N and 60°S; therefore, the total area for the Arctic realm is an underestimate. For the Southern Ocean, there are no records of tidal marshes on mainland Antarctica (Greenberg et al., 2006), and our map does not classify any of the limited coastal wetlands on the sub-Antarctic islands as tidal marshes.
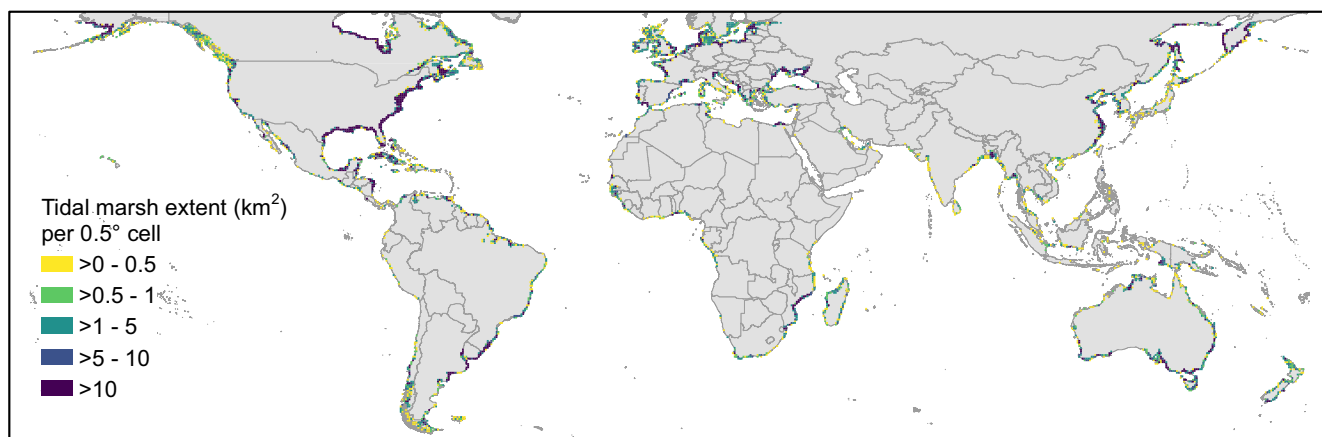

Tidal marsh extent (km^2) per 0.5° cell
- >0 - 0.5
- >0.5 - 1
- >1 - 5
- >5 - 10
- >10

FIGURE 1 The 2020 distribution of tidal marshes, with darker colours representing greater extents of tidal marshes (km^2) within a 0.5° grid cell.

Our map indicated tropical realms support 7410 km^2 (CI: 4450 to 8380 km^2) of tidal marshes. In the tropics, coastal wetlands are typically dominated by mangroves; however, tidal marshes are still found in most areas (e.g. Almahasheer, 2021; Hena et al., 2007; Viswanathan et al., 2020), albeit often within spatially confined areas. Viswanathan et al. (2020) estimated 290 km^2 of 'salt marsh' around the coast of India, considerably more than the 50 km^2 from our analysis; however, the density of salt marsh vegetation in the Indian study (19 ± 1 plants per m^2) was lower than the average density of tidal marshes in temperate regions, highlighting the challenge of identifying tidal marshes with different structures in different regions of the world. Within the Indo-Pacific Realms, our maps show a larger distribution of tidal marsh around the coasts of Mozambique, Madagascar and northern Australia. These are somewhat arid macrotidal regions where tidal marshes typically occur behind mangroves, high in the tidal frame (Saintilan, 2009). In the Tropical Atlantic, tidal marshes are widespread—notably in Central America and Cuba—again in close proximity to mangroves, and usually in the upper reaches of the tidal frame.

3.2 | National estimates

Political contexts set the scene for conservation action and hence understanding distribution and spatial statistics at national levels is important. Such information also serves to provide data for National Biodiversity Strategies and Action Plans and the United Nations' System of Environmental-Economic Accounting. Our map identifies
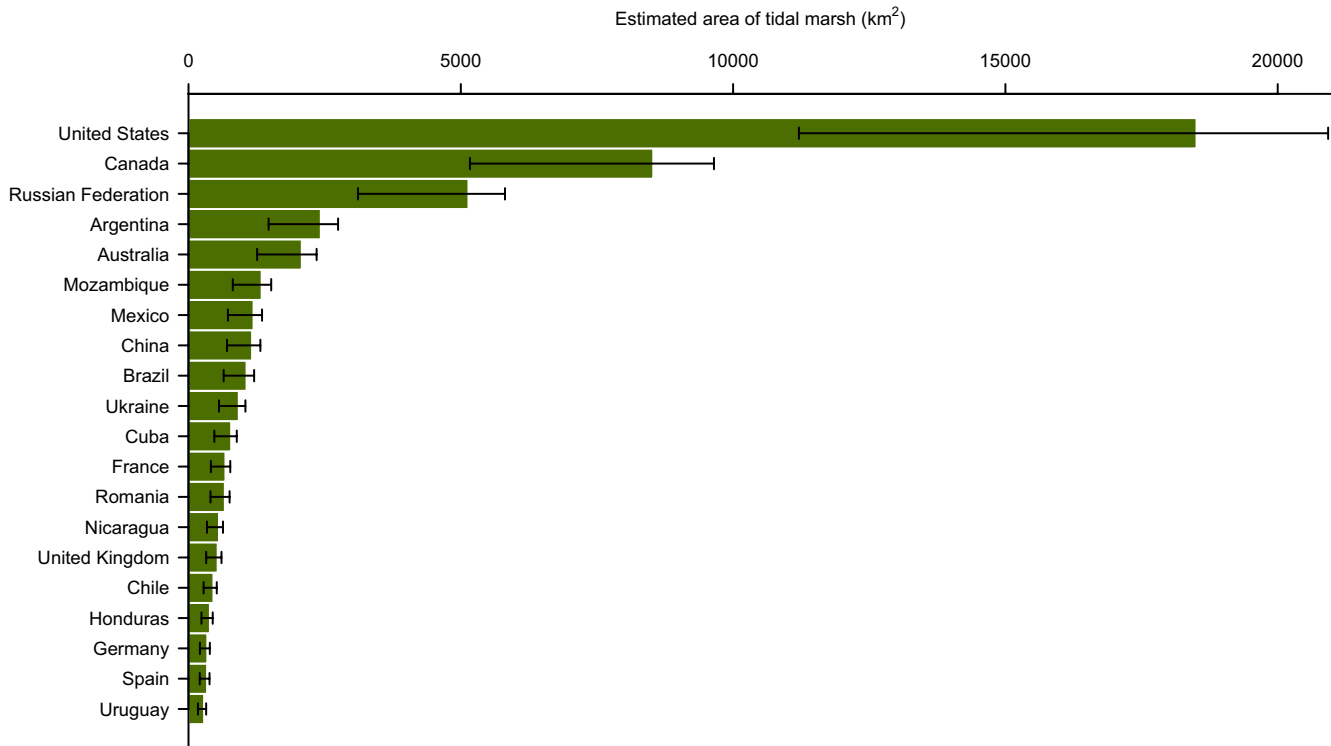
FIGURE 2 The area of tidal marsh in the countries with the largest extents. 95% confidence intervals were estimated by resampling the validation set ($n = 1000$) and using the 0.05 percentile of the commission and omission error estimates. The resampling procedure allowed for asymmetry in the confidence intervals around our tidal marsh extent estimates, which better represent the unevenness in the omission and commission errors identified in our map.

tidal marsh ecosystems in 120 countries, and Figure 2 shows the extents for the 20 countries with the largest areas of tidal marsh. At the national scale, over a third of the global extent (18,510 km^2; CI: 11,210–20,930) is estimated to be found within the U.S.A. (Figure 2), with tidal marshes across all coastlines, but most extensive on the Atlantic and Gulf of Mexico coasts. Canada (8530 km^2; CI: 5170–9650) and Russia (5140 km^2; CI: 3110–5810) are also important, and the combined extent of just these three countries makes up over 60% of global tidal marsh extent. Any future inclusion of data from above 60° N would further highlight this dominance. An additional six countries are estimated to have tidal marsh extents in excess of 1000 km^2 (Supporting Information Table S6).

In Europe, tidal marshes are extensive, with a combined total of ~5000 km^2, concentrated along the Atlantic coasts, the North and Baltic Seas. With its microtidal regime, and influenced by millennia of human conversion (Airoldi & Beck, 2007), the Mediterranean has only limited tidal marsh areas and many are fragmented. Our maps also show tidal marsh in the northern Black Sea, particularly in the major river deltas of the Danube and Dnepr and along the eastern shore of the Azov Sea (Figure 1).

3.3 | Comparison to other global estimates

While our total extent closely matches the global estimate of Mcowen et al. (2017; 54,951 km^2), there are notable differences in

the distribution between the two maps. We identify tidal marshes in an extra 17 countries, while our maps include spatial extents for a further 71 countries where Mcowen et al. (2017) provide only point locations. Our extent is also in line with a 45,000 km^2 estimate for non-arctic tidal marshes (Greenberg et al., 2006). However, our extent is 58–71% of the estimates of Murray, Worthington, et al. (90,800 km^2; 2022) and Zhang et al. (74,910 km^2; 2023) respectively. The former was a more broadly based study of intertidal wetland dynamics and thus not directly comparable. Zhang et al. (2023) is a lower resolution (30 m) global assessment of all wetlands, which includes "coastal saltmarsh". The larger extent predicted is somewhat explained by the inclusion of 4800 km^2 along Arctic coastlines which were precluded from our study (see below). In addition, the study of Zhang et al. (2023) predicts the presence of "coastal saltmarsh" over a far greater proportion of the global coastline; however, this is partly explained by the fact that it does not apply an area filter to remove the noise (predictions of wetland distribution confined to single pixels) in their maps. No recent maps have come close to the highest previous global estimates of 400,000 km^2 (Duarte et al., 2005).

The strength of our approach is that it was targeted to the mapping of tidal marshes using training sets that conform to a single class definition (e.g. Keith et al., 2022) and was developed via deep literature review and image interpretation. The image covariates were designed for the purpose of mapping tidal marshes (not all wetlands), and underpin a classification approach shown to perform well in

coastal environments which is essential for resolving the uncertainty in tidal marsh distribution.

3.4 | Protected areas

We estimate that over 45% (24,200 km^2) of the world's 52,880 km^2 of tidal marshes are found within the boundaries of protected areas. This is approximately equivalent to the extent of mangroves that occur within protected areas (42%; Leal & Spalding, 2022) and greater than the current area of coral reefs (32%; Marine Conservation Institute, 2018) or tidal flats (31%; Hill et al., 2021). Such extensive protection of coastal ecosystems likely reflects a growing perception of their immense value for biodiversity and for people. In this regard, tidal marshes are among the few ecosystem types globally that already met the 30% protection threshold of Target 3 of the Kunming–Montreal Global Biodiversity Framework; however, other aspects of Target 3 such as protected areas being effectively managed, well-connected and equitably governed are yet to be fully assessed (CBD, 2022). Further, it is important to be aware that if we could measure original tidal marsh extent, this figure would be considerably lower. The USA and Canada are critical in securing these levels of coverage with some 6600 and 3500 km^2 in protected areas, or 35% and 41% of their national tidal marsh extent respectively (Figure 3). In Europe, the proportional coverage is particularly high, with 14 European countries having >90% of their extant tidal marshes within their protected area network (Figure 3; Supporting Information Table S6), although it is noteworthy that our knowledge of losses in this region suggests that most countries have lost between 50% and 90% of historical cover (Airoldi & Beck, 2007).

3.5 | Challenges and limitations

One of the main challenges in developing a global map of tidal marshes is the considerable variability in an ecosystem that is globally distributed, ranging from monospecific reedbeds, salt-tolerant grasses and low, succulent shrubs, and that exists under highly variable environmental settings (Keith et al., 2022). The habitats captured in our analysis maps are highly diverse: many are extensive near-continuous areas dominating the upper reaches of wide intertidal frames. Elsewhere they are part of a tight mosaic with other habitats such as mangroves in tropical regions, or in complexes of dunes, lakes, marshes and drylands in the higher latitudes. In most areas, tidal flushing is likely to be regular, but in some settings, such as in microtidal regimes, and in intermittently closed and open lagoons, such inundation may be more seasonal or intermittent.

In large part, the tidal marshes in our maps conform to the definition of salt marsh developed by Adam (2002), which is close to that of Keith et al. (2022) for "Coastal saltmarshes and reedbeds". By contrast, the Ramsar Convention recognizes several habitat types within tidal marshes including salt marshes, salt meadows, saltings, tidal brackish and freshwater marshes (Department of Climate Change Energy the Environment and Water, 2021). Even so, any mapping practice of this sort is, in part, constrained by what can be distinguished remotely from imagery or associated interpretation. In this study, our mapped distribution includes a considerable number of brackish to freshwater tidal marshes alongside the more strongly halophytic communities that have been described by others. This is a potential limitation of the research as it is currently not possible to differentiate such systems based on salinity using remote sensing methods; however,
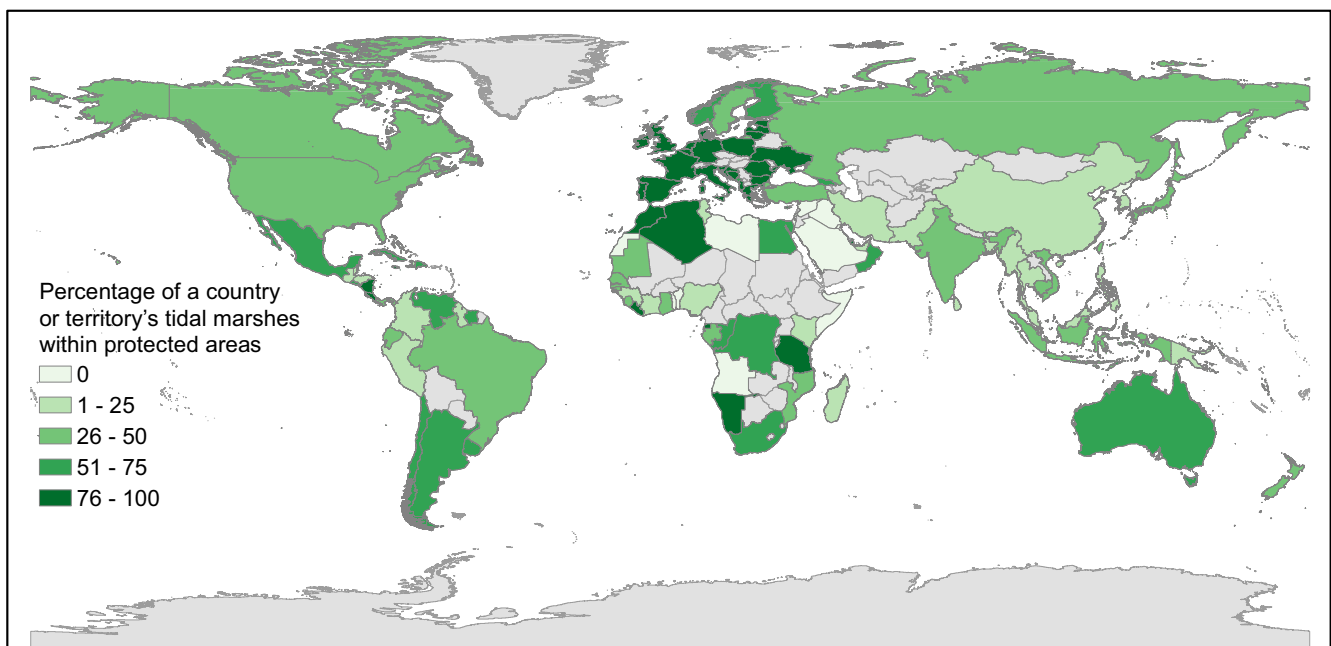

FIGURE 3 The percentage of the country or territory's tidal marsh extent within the boundaries of a protected area.

it ensures that we incorporate the entirety of an ecotone that is rarely, if ever, a sharp boundary (Maltby & Barker, 2009; Phelan et al., 2011).

The use of a global training dataset (Murray, Bunting, et al., 2022) was intended to include tidal marsh ecosystems present across all latitudes and representing very different tidal and climatic regimes; however, training data for the model were most comprehensive in areas where more tidal marshes occur, primarily temperate regions. This resulted in a potential bias in our prediction towards tidal marshes with physical features reflected by the training set and, aside from showing the distributional range of tidal marshes, it is noteworthy that our map also shows gaps—stretches of coastlines or regions where tidal marshes are rare to absent. These include many oceanic islands, but also some wet tropical regions in Southeast Asia. Gaps associated with hypersaline flats of northern Australia and the Middle East are also notable—these areas may have sparse salt marsh plants fringing the margins of sabkha ecosystems (Barth & Böer, 2002), but these areas of very sparse fringing marsh vegetation were specifically not included in the training set.

Assessment of the accuracy of our map indicated greater commission errors in comparison to omissions errors (see also Murray, Worthington, et al., 2022), with high values in many tropical regions (Table 1). This highlights that our analysis is overpredicting tidal marsh presence (false positives), with the errors particularly prevalent in those areas lacking extensive data for model training (see above). Visual assessment of the map identified the chief causes of these false positives were human modification of the coastal zone for aquaculture and flooded agriculture such as rice fields, while in northern latitudes rocky shorelines proved challenging for the classifier. While manual correction removed many of these misclassifications, errors will still persist in the final product.

The latitudinal limits to our study do not affect the southern hemisphere where tidal marsh is thought not to occur on the Antarctic continent (Greenberg et al., 2006); however, they mean we underestimate the overall tidal marsh extent in the Arctic. Our map covers the southern parts of the Arctic realm in Canada, USA and Russia, the areas that are likely to host a large proportion of arctic tidal marshes because they are less impacted by extreme conditions of temperature, snow and ice cover, ice scour, high wave energy and isostatic uplift compared to the higher latitude coasts. Despite the gap in our coverage, the very large areas we show, notably in southern Baffin Bay in Canada, mean that this realm has the second highest tidal marsh coverage, globally. Moving north, beyond the reach of our maps, it is likely that tidal marshes will be less extensive owing to the impact of ice abrasion and the harsh climate (Adam, 2002; Scott et al., 2014a). Zhang et al. (2023) map 4800 km^2 in the high Arctic area; however, given the differences in our mapping approaches, we would predict a much smaller extent than this in these high latitudes. It is important to note that while the tidal marshes in these high northern latitudes tend to be limited in distribution with low diversity, they are extremely vulnerable to environmental change (Adam, 1990, 2002; Chapman, 1974; Martini et al., 2019; Sergienko, 2013).

4 | CONCLUSIONS

This research presents the first consistent medium-resolution tidal marsh distribution map for the world. Compared to previous studies, it identifies tidal marshes in more countries and across a greater proportion of the world's coastline and provides the higher resolution view of the extant distribution of this globally widespread coastal ecosystem. While there are opportunities to improve the map, particularly in the high Arctic and some tropical and arid regions, it already provides an invaluable baseline against which to measure change and to quantify the value of important ecosystem services.

Historic losses of tidal marshes have been considerable, with some areas continuing to experience land use conversion and tidal marsh degradation. With a globally consistent method that focuses solely on tidal marshes to develop a strong baseline, it should be possible to use our map to identify recent losses, following the methods established for wetland ecosystems (Bunting et al., 2022; Campbell et al., 2022; Murray, Worthington, et al., 2022). Our map will, therefore, enable better tracking of ongoing changes, which may represent natural dynamics, the impacts of sea level rise (Saintilan et al., 2022) or direct human modifications including tidal marsh conversion or the impact of marsh restoration efforts (Murray, Worthington, et al., 2022). Other work is ongoing to better quantify the carbon stocks in tidal marsh soils (e.g. Maxwell et al., 2023) and coastal protection functions, while it is hoped that others may be able to develop improved maps of fisheries enhancement and other benefits. Tidal marshes, although spatially limited, represent ecosystems of critical importance to biodiversity and to people. By establishing an open-access, global baseline, we hope to encourage greater efforts to secure a long-term future for these ecosystems, and indeed for the millions of people who depend upon them.

CONFLICT OF INTEREST STATEMENT

The authors declare that they have no conflict of interest.

DATA AVAILABILITY STATEMENT

The tidal marsh distribution data are viewable at https://tomworthington81.users.earthengine.app/view/global-tidal-marsh-distribution and made available directly via Google Earth Engine (Asset ID: users/tomworthington81/SM_Global_2020/global_export_v2_6/saltmarsh_v2_6). Raster tiles of the entire tidal marsh extent can be downloaded from https://doi.org/10.5281/zenodo.8420753.

ORCID

Thomas A. Worthington https://orcid.org/0000-0002-8138-9075

REFERENCES

Achanta, R., & Süsstrunk, S. (2017). Superpixels and polygons using simple non-iterative clustering. In *2017 IEEE Conference on Computer Vision and Pattern Recognition (CVPR)* (pp. 4895–4904). IEEE.

Adam, P. (1990). Saltmarsh ecology. In *Cambridge studies in ecology: Saltmarsh ecology.* Cambridge University Press.

Adam, P. (2002). Saltmarshes in a time of change. *Environmental Conservation*, 29(1), 39–61.

Adams, J. B. (2020). Salt marsh at the tip of Africa: Patterns, processes and changes in response to climate change. *Estuarine, Coastal and Shelf Science*, 237, 106650.

Airoldi, L., & Beck, M. W. (2007). Loss, status and trends for coastal marine habitats of Europe. *Oceanography and Marine Biology: An Annual Review*, 45, 345–405.

Allen, J. R. L. (2000). Morphodynamics of Holocene salt marshes: A review sketch from the Atlantic and Southern North Sea coasts of Europe. *Quaternary Science Reviews*, 19(12), 1155–1231.

Almahasheer, H. (2021). Assessment of coastal salt marsh plants on the Arabian Gulf region. *Saudi Journal of Biological Sciences*, 28(10), 5640–5646.

Almeida, D., Neto, C., Esteves, L. S., & Costa, J. C. (2014). The impacts of land-use changes on the recovery of saltmarshes in Portugal. *Ocean and Coastal Management*, 92, 40–49.

Amante, C., & Eakins, B. W. (2009). ETOPO1 1 arc-minute global relief model: Procedures, data sources and analysis. In *NOAA Technical Memorandum NESDIS NGDC-24*. National Ocean and Atmospheric Administration.

Baker, R., Taylor, M. D., Able, K. W., Beck, M. W., Cebrian, J., Colombano, D. D., Connolly, R. M., Currin, C., Deegan, L. A., Feller, I. C., Gilby, B. L., Kimball, M. E., Minello, T. J., Rozas, L. P., Simenstad, C., Eugene Turner, R., Waltham, N. J., Weinstein, M. P., Ziegler, S. L., … Staver, L. W. (2020). Fisheries rely on threatened salt marshes. *Science*, 370(6517), 670–671.

Barbier, E. B., Hacker, S. D., Kennedy, C., Koch, E. W., Stier, A. C., & Silliman, B. R. (2011). The value of estuarine and coastal ecosystem services. *Ecological Monographs*, 81(2), 169–193.

Barendregt, A. (2018). Tidal freshwater wetlands: The fresh dimension of the estuary. In C. M. Finlayson, G. R. Milton, R. C. Prentice, & N. C. Davidson (Eds.), *The wetland book: II: Distribution, description, and conservation* (pp. 155–168). Springer.

Barth, H.-J., & Böer, B. (Eds.). (2002). *Sabkha ecosystems. Volume I: The Arabian Peninsula and adjacent countries*. Springer.

Belgiu, M., & Drăgu, L. (2016). Random forest in remote sensing: A review of applications and future directions. *ISPRS Journal of Photogrammetry and Remote Sensing*, 114, 24–31.

Berger, M., Moreno, J., Johannessen, J. A., Levelt, P. F., & Hanssen, R. F. (2012). ESA's sentinel missions in support of Earth system science. *Remote Sensing of Environment*, 120, 84–90.

Bunting, P. (2020). Class accuracy. https://github.com/remotesensinginfo/classaccuracy

Bunting, P., Rosenqvist, A., Hilarides, L., Lucas, R. M., Thomas, N., Tadono, T., Worthington, T. A., Spalding, M., Murray, N. J., & Rebelo, L.-M. (2022). Global mangrove extent change 1996-2020: Global Mangrove Watch version 3.0. *Remote Sensing*, 14(15), 3657.

Bunting, P., Rosenqvist, A., Lucas, R., Rebelo, L.-M., Hilarides, L., Thomas, N., Hardy, A., Itoh, T., Shimada, M., & Finlayson, C. (2018). The Global Mangrove Watch—A new 2010 global baseline of mangrove extent. *Remote Sensing*, 10(10), 1669.

Campbell, A. D., Fatoyinbo, L., Goldberg, L., & Lagomasino, D. (2022). Global hotspots of salt marsh change and carbon emissions. *Nature*, 612(7941), 701–706.

Cavanaugh, K. C., Dangremond, E. M., Doughty, C. L., Williams, A. P., Parker, J. D., Hayes, M. A., Rodriguez, W., & Feller, I. C. (2019). Climate-driven regime shifts in a mangrove–salt marsh ecotone over the past 250 years. *Proceedings of the National Academy of Sciences*, 116(43), 21602–21608.

Cavanaugh, K. C., Kellner, J. R., Forde, A. J., Gruner, D. S., Parker, J. D., Rodriguez, W., & Feller, I. C. (2014). Poleward expansion of mangroves is a threshold response to decreased frequency of extreme cold events. *Proceedings of the National Academy of Sciences of the United States of America*, 111(2), 723–727.

CBD. (2022). The Kunming-Montreal global biodiversity framework. https://www.cbd.int/doc/c/e6d3/cd1d/daf663719a03902a9b116c34/cop-15-l-25-en.pdf

Chapman, V. J. (1974). *Salt marshes and salt deserts of the world*. Verlag von J Cramer.

Chmura, G. L., Anisfeld, S. C., Cahoon, D. R., & Lynch, J. C. (2003). Global carbon sequestration in tidal, saline wetland soils. *Global Biogeochemical Cycles*, 17(4), 1111.

Costanza, R., Pérez-Maqueo, O., Martinez, M. L., Sutton, P., Anderson, S. J., & Mulder, K. (2008). The value of coastal wetlands for hurricane protection. *Ambio*, 37(4), 241–248.

Cutler, D. R., Edwards, T. C., Beard, K. H., Cutler, A., Hess, K. T., Gibson, J., & Lawler, J. J. (2007). Random forests for classification in ecology. *Ecology*, 88(11), 2783–2792.

Davy, A. J., Bakker, J. P., & Figueroa, M. E. (2009). Human modification of European salt marshes. In B. R. Silliman, T. Grosholzand, & M. D. Bertness (Eds.), *Human impacts on salt marshes: A global perspective* (pp. 311–336). University of California Press.

Department of Climate Change Energy the Environment and Water. (2021). Ramsar wetland type classification. https://www.environment.gov.au/water/wetlands/ramsar/wetland-type-classification

Dormann, C. F., Elith, J., Bacher, S., Buchmann, C., Carl, G., Carré, G., Marquéz, J. R. G., Gruber, B., Lafourcade, B., Leitão, P. J., Münkemüller, T., Mcclean, C., Osborne, P. E., Reineking, B., Schröder, B., Skidmore, A. K., Zurell, D., & Lautenbach, S. (2013). Collinearity: A review of methods to deal with it and a simulation study evaluating their performance. *Ecography*, 36(1), 27–46.

Duarte, C. M., Middelburg, J. J., & Caraco, N. (2005). Major role of marine vegetation on the oceanic carbon cycle. *Biogeosciences*, 2, 1–8.

Elvidge, C. D., Baugh, K., Zhizhin, M., Hsu, F. C., & Ghosh, T. (2017). VIIRS night-time lights. *International Journal of Remote Sensing*, 38(21), 5860–5879.

Feyisa, G. L., Meilby, H., Fensholt, R., & Proud, S. R. (2014). Automated Water Extraction Index: A new technique for surface water mapping using Landsat imagery. *Remote Sensing of Environment*, 140, 23–35.

Flanders Marine Institute. (2020). Union of the ESRI Country shapefile and the Exclusive Economic Zones (version 3). https://www.marineregions.org/

Friess, D. A., Yando, E. S., Alemu, J. B., Wong, L.-W., Soto, S. D., & Bhatia, N. (2020). Ecosystem services and disservices of mangrove forests and salt marshes. *Oceanography and Marine Biology*, 58, 107–142.

Fu, B., He, X., Yao, H., Liang, Y., Deng, T., He, H., Fan, D., Lan, G., & He, W. (2022). Comparison of RFE-DL and stacking ensemble learning algorithms for classifying mangrove species on UAV multispectral images. *International Journal of Applied Earth Observation and Geoinformation*, 112, 102890.

Gedan, K. B., & Silliman, B. R. (2009). Patterns of salt marsh loss within coastal regions of North America: Presettlement to present. In B. R. Silliman, T. Grosholzand, & M. D. Bertness (Eds.), *Human impacts on salt marshes: A global perspective* (pp. 253–265). University of California Press.

Giri, C., Ochieng, E., Tieszen, L. L., Zhu, Z., Singh, A., Loveland, T., Masek, J., & Duke, N. (2011). Status and distribution of mangrove forests of the world using Earth observation satellite data. *Global Ecology and Biogeography*, 20(1), 154–159.

Gorelick, N., Hancher, M., Dixon, M., Ilyushchenko, S., Thau, D., & Moore, R. (2017). Google Earth Engine: Planetary-scale geospatial analysis for everyone. *Remote Sensing of Environment, 202*, 18–27.

Greenberg, R., Maldonado, J. E., Droege, S., McDonald, M. V., & Donald, M. V. M. C. (2006). Tidal marshes: A global perspective on the evolution and conservation of their terrestrial vertebrates. *Bioscience, 56*(8), 675–685.

Gu, J., Luo, M., Zhang, X., Christakos, G., Agusti, S., Duarte, C. M., & Wu, J. (2018). Losses of salt marsh in China: Trends, threats and management. *Estuarine, Coastal and Shelf Science, 214*, 98–109.

Hanson, J. O. (2022). Wdpar: Interface to the world database on protected areas. *Journal of Open Source Software, 7*(78), 4594.

Hatje, V., Copertino, M., Patire, V. F., Ovando, X., Ogbuka, J., Johnson, B. J., Kennedy, H., Masque, P., & Creed, J. C. (2023). Vegetated coastal ecosystems in the Southwestern Atlantic Ocean are an unexploited opportunity for climate change mitigation. *Communications Earth & Environment, 4*(1), 1–10.

Hena, M. K. A., Short, F. T., Sharifuzzaman, S. M., Hasan, M., Rezowan, M., & Ali, M. (2007). Salt marsh and seagrass communities of Bakkhali Estuary, Cox's Bazar, Bangladesh. *Estuarine, Coastal and Shelf Science, 75*(1–2), 72–78.

Hill, N. K., Woodworth, B. K., Phinn, S. R., Murray, N. J., & Fuller, R. A. (2021). Global protected-area coverage and human pressure on tidal flats. *Conservation Biology, 35*(3), 933–943.

Hopkinson, C. S., Cai, W. J., & Hu, X. (2012). Carbon sequestration in wetland dominated coastal systems—A global sink of rapidly diminishing magnitude. *Current Opinion in Environmental Sustainability, 4*(2), 186–194.

Hu, Y., Tian, B., Yuan, L., Li, X., Huang, Y., Shi, R., Jiang, X., Wang, L., & Sun, C. (2021). Mapping coastal salt marshes in China using time series of Sentinel-1 SAR. *ISPRS Journal of Photogrammetry and Remote Sensing, 173*, 122–134.

Huete, A., Didan, K., Miura, T., Rodriguez, E. P., Gao, X., & Ferreira, L. G. (2002). Overview of the radiometric and biophysical performance of the MODIS vegetation indices. *Remote Sensing of Environment, 83*(1–2), 195–213.

Isacch, J. P., Costa, C. S. B., Rodriguez-Gallego, L., Conde, D., Escapa, M., Gagliardini, D. A., & Iribarne, O. O. (2006). Distribution of saltmarsh plant communities associated with environmental factors along a latitudinal gradient on the south-west Atlantic coast. *Journal of Biogeography, 33*, 888–900.

Jänes, H., Macreadie, P. I., Zu Ermgassen, P. S. E., Gair, J. R., Treby, S., Reeves, S., Nicholson, E., Ierodiaconou, D., & Carnell, P. (2020). Quantifying fisheries enhancement from coastal vegetated ecosystems. *Ecosystem Services, 43*, 101105.

Keith, D. A., Ferrer-Paris, J. R., Nicholson, E., Bishop, M. J., Polidoro, B. A., Ramirez-Llodra, E., Tozer, M. G., Nel, J. L., Mac Nally, R., Gregr, E. J., Watermeyer, K. E., Essl, F., Faber-Langendoen, D., Franklin, J., Lehmann, C. E. R., Etter, A., Roux, D. J., Stark, J. S., Rowland, J. A., ... Kingsford, R. T. (2022). A function-based typology for Earth's ecosystems. *Nature, 610*(7932), 513–518.

Kuenzer, C., Bluemel, A., Gebhardt, S., Quoc, T. V., & Dech, S. (2011). Remote sensing of mangrove ecosystems: A review. *Remote Sensing, 3*(5), 878–928.

Kuhn, M. (2021). caret: Classification and regression training. R package version 6.0-88 https://CRAN.R-project.org/package=caret

Leal, M., & Spalding, M. D. (2022). *The state of the world's mangroves 2022*. Global Mangrove Alliance.

Li, J., Knapp, D. E., Fabina, N. S., Kennedy, E. V., Larsen, K., Lyons, M. B., Murray, N. J., Phinn, S. R., Roelfsema, C. M., & Asner, G. P. (2020). A global coral reef probability map generated using convolutional neural networks. *Coral Reefs, 39*(6), 1805–1815.

Lopez-Portillo, J., & Ezcurra, E. (1989). Zonation in mangrove and salt marsh vegetation at Laguna de Mecoacan, Mexico. *Biotropica, 21*(2), 107–114.

Lyons, M. B., Keith, D. A., Phinn, S. R., Mason, T. J., & Elith, J. (2018). A comparison of resampling methods for remote sensing classification and accuracy assessment. *Remote Sensing of Environment, 208*, 145–153.

Lyons, M. B., Roelfsema, C. M., Kennedy, E. V., Kovacs, E. M., Borrego-Acevedo, R., Markey, K., Roe, M., Yuwono, D. M., Harris, D. L., Phinn, S. R., Asner, G. P., Li, J., Knapp, D. E., Fabina, N. S., Larsen, K., Traganos, D., & Murray, N. J. (2020). Mapping the world's coral reefs using a global multiscale Earth observation framework. *Remote Sensing in Ecology and Conservation, 6*(4), 557–568.

Main-Korn, M., Pflug, B., Louis, J., Debaecker, V., Müller-Wilm, U., & Gascon, F. (2017). Sen2Cor for Sentinel-2. In *Proceedings Volume 10427, Image and Signal Processing for Remote Sensing XXIII* (1042704). SPIE Remote Sensing.

Mahdianpari, M., Salehi, B., Mohammadimanesh, F., Homayouni, S., & Gill, E. (2019). The first wetland inventory map of Newfoundland at a spatial resolution of 10 m using sentinel-1 and sentinel-2 data on the Google Earth Engine cloud computing platform. *Remote Sensing, 11*, 43.

Maltby, E., & Barker, M. T. (2009). *The wetlands handbook*. Wiley-Blackwell.

Marine Conservation Institute. (2018). Status Watch: How Well Are Coral Reefs Protected Around the World? https://marine-conservation.org/on-the-tide/how-well-are-coral-reefs-protected/

Martini, I. P., Morrison, R. I. G., Abraham, K. F., Sergienko, L. A., & Jefferies, R. L. (2019). Northern polar coastal wetlands: Development, structure, and land use. In G. M. E. Perillo, E. Wolanski, D. R. Cahoon, & C. S. Hopkinson (Eds.), *Coastal wetlands: An integrated ecosystem approach* (pp. 153–186). Elsevier.

Maxwell, T. L., Rovai, A. S., Adame, M. F., Adams, J. B., Álvarez-Rogel, J., Austin, W. E. N., Beasy, K., Boscutti, F., Böttcher, M. E., Bouma, T. J., Bulmer, R. H., Burden, A., Burke, S. A., Camacho, S., Chaudhary, D. R., Chmura, G. L., Copertino, M., Cott, G. M., Craft, C., ... Worthington, T. A. (2023). Global dataset of soil organic carbon in tidal marshes. *Scientific Data, 10*(1), 797.

McLeod, E., Chmura, G. L., Bouillon, S., Salm, R., Björk, M., Duarte, C. M., Lovelock, C. E., Schlesinger, W. H., & Silliman, B. R. (2011). A blueprint for blue carbon: Toward an improved understanding of the role of vegetated coastal habitats in sequestering CO_2. *Frontiers in Ecology and the Environment, 9*(10), 552–560.

Mcowen, C. J., Weatherdon, L. V., Van Bochove, J. W., Sullivan, E., Blyth, S., Zockler, C., Stanwell-Smith, D., Kingston, N., Martin, C. S., Spalding, M., & Fletcher, S. (2017). A global map of saltmarshes. *Biodiversity Data Journal, 5*(1), e11764.

Melville, D. S., Chen, Y., & Ma, Z. (2016). Shorebirds along the Yellow Sea coast of China face an uncertain future—A review of threats. *Emu, 116*(2), 100–110.

Mitsch, W. J., & Gosselink, J. G. (2015). *Wetlands*. John Wiley & Sons, Inc.

Möller, I., Kudella, M., Rupprecht, F., Spencer, T., Paul, M., Van Wesenbeeck, B. K., Wolters, G., Jensen, K., Bouma, T. J., Miranda-Lange, M., & Schimmels, S. (2014). Wave attenuation over coastal salt marshes under storm surge conditions. *Nature Geoscience, 7*(10), 727–731.

Murray, N. J., Bunting, P., Canto, R. F., Hilarides, L., Kennedy, E. V., Lucas, R. M., Lyons, M. B., Navarro, A., Roelfsema, C. M., Rosenqvist, A., Spalding, M. D., Toor, M., & Worthington, T. A. (2022). coastTrain: A global reference library for coastal ecosystems. *Remote Sensing, 14*(22), 5766.

Murray, N. J., Phinn, S. R., DeWitt, M., Ferrari, R., Johnston, R., Lyons, M. B., Clinton, N., Thau, D., & Fuller, R. A. (2019). The global distribution and trajectory of tidal flats. *Nature, 565*(7738), 222–225.

Murray, N. J., Worthington, T. A., Bunting, P., Duce, S., Hagger, V., Lovelock, C. E., Lucas, R., Saunders, M. I., Sheaves, M., Spalding, M., Waltham, N. J., & Lyons, M. B. (2022). High-resolution mapping of losses and gains of Earth's tidal wetlands. *Science, 376*(6594), 744–749.

Narayan, S., Beck, M. W., Wilson, P., Thomas, C. J., Guerrero, A., Shepard, C. C., Reguero, B. G., Franco, G., Ingram, J. C., & Trespalacios, D. (2017). The value of coastal wetlands for flood

damage reduction in the Northeastern USA. *Scientific Reports*, *7*, 9463.

Neumann, B., Vafeidis, A. T., Zimmermann, J., & Nicholls, R. J. (2015). Future coastal population growth and exposure to sea-level rise and coastal flooding—A global assessment. *PLoS ONE*, *10*(6), e0131375.

Nicodemus, K. K., & Malley, J. D. (2009). Predictor correlation impacts machine learning algorithms: Implications for genomic studies. *Bioinformatics*, *25*(15), 1884–1890.

Pendleton, L., Donato, D. C., Murray, B. C., Crooks, S., Jenkins, W. A., Sifleet, S., Craft, C., Fourqurean, J. W., Kauffman, J. B., Marbà, N., Megonigal, P., Pidgeon, E., Herr, D., Gordon, D., & Baldera, A. (2012). Estimating global "blue carbon" emissions from conversion and degradation of vegetated coastal ecosystems. *PLoS ONE*, *7*(9), e43542.

Pettorelli, N., Vik, J. O., Mysterud, A., Gaillard, J.-M. M., Tucker, C. J., & Stenseth, N. C. (2005). Using the satellite-derived NDVI to assess ecological responses to environmental change. *Trends in Ecology & Evolution*, *20*(9), 503–510.

Phelan, N., Shaw, A., & Baylis, A. (2011). *The extent of saltmarsh in England and Wales: 2006–2009*. Environment Agency.

R Core Team. (2023). *R: A language and environment for statistical computing (4.3.2)*. R Foundation for Statistical Computing. https://www.r-project.org/

Rodriguez, W., Feller, I. C., & Cavanaugh, K. C. (2016). Spatio-temporal changes of a mangrove–saltmarsh ecotone in the northeastern coast of Florida, USA. *Global Ecology and Conservation*, *7*, 245–261.

Saintilan, N. (2009). Distribution of Australian saltmarsh plants. In N. Saintilan (Ed.), *Australian saltmarsh ecology* (pp. 23–39). CSIRO.

Saintilan, N., Kovalenko, K. E., Guntenspergen, G., Rogers, K., Lynch, J. C., Cahoon, D. R., Lovelock, C. E., Friess, D. A., Ashe, E., Krauss, K. W., Cormier, N., Spencer, T., Adams, J., Raw, J., Ibanez, C., Scarton, F., Temmerman, S., Meire, P., Maris, T., ... Khan, N. (2022). Constraints on the adjustment of tidal marshes to accelerating sea level rise. *Science*, *377*(6605), 523–527.

Schuerch, M., Spencer, T., Temmerman, S., Kirwan, M. L., Wolff, C., Lincke, D., McOwen, C. J., Pickering, M. D., Reef, R., Vafeidis, A. T., Hinkel, J., Nicholls, R. J., & Brown, S. (2018). Future response of global coastal wetlands to sea-level rise. *Nature*, *561*(7722), 231–234.

Schultz, M., Clevers, J. G. P. W., Carter, S., Verbesselt, J., Avitabile, V., Quang, H. V., & Herold, M. (2016). Performance of vegetation indices from Landsat time series in deforestation monitoring. *International Journal of Applied Earth Observation and Geoinformation*, *52*, 318–327.

Scott, D. B., Frail-Gauthier, J., & Mudie, P. J. (2014a). Coastal wetlands worldwide: Climatic zonation, ecosystems and biogeography. In *Coastal wetlands of the world: Geology, ecology, distribution and applications* (pp. 57–71). Cambridge University Press.

Scott, D. B., Frail-Gauthier, J., & Mudie, P. J. (2014b). Physical aspects: Geological, oceanic and climatic conditions. In *Coastal wetlands of the world: Geology, ecology, distribution and applications* (pp. 5–16). Cambridge University Press.

Sergienko, L. (2013). Salt marsh flora and vegetation of the Russian Arctic coasts. *Czech Polar Reports*, *3*(1), 30–37.

Shepard, C. C., Crain, C. M., & Beck, M. W. (2011). The protective role of coastal marshes: A systematic review and meta-analysis. *PLoS ONE*, *6*(11), e27374.

Shi-lun, Y., & Ji-yu, C. (1995). Coatal salt marshes and mangrove swamps in China. *Chinese Journal of Oceanology and Limnology*, *13*(4), 318–324.

Silliman, B. R., Van Koppel, J. D., Bertness, M. D., Stanton, L. E., & Mendelssohn, I. A. (2005). Drought, snails, and large-scale die-off of Southern U.S. salt marshes. *Science*, *310*(5755), 1803–1806.

Spalding, M. D., Fox, H. E., Allen, G. R., Davidson, N., Ferdaña, Z. A., Finlayson, M., Halpern, B. S., Jorge, M. A., Lombana, A., Lourie, S. A., Martin, K. D., McManus, E., Molnar, J., Recchia, C. A., & Robertson, J. (2007). Marine ecoregions of the world: A bioregionalization of coastal and shelf areas. *Bioscience*, *57*(7), 573–583.

Tiner, R. W., & Milton, G. R. (2018). Estuarine marsh: An overview. In C. M. Finlayson, G. R. Milton, R. C. Prentice, & N. C. Davidson (Eds.), *The wetland book: II: Distribution, description, and conservation* (pp. 55–72). Springer.

U.S. Fish and Wildlife Service. (2021). *National Wetlands Inventory website*. U.S. Department of the Interior, Fish and Wildlife Service.

UNEP-WCMC and IUCN. (2023). *Protected planet: The world database on protected areas (WDPA)* [Online], May 2023. UNEP-WCMC and IUCN. www.protectedplanet.net

Veci, L., Prats-Iraola, P., Scheiber, R., Collard, F., Fomferra, N., & Engdahl, M. (2014). The Sentinel-1 toolbox. In *Proceedings of the IEEE International Geoscience and Remote Sensing Symposium (IGARSS)* (pp. 1–3). IEEE.

Viswanathan, C., Purvaja, R., Jeevamani, J. J., Deepak Samuel, V., Sankar, R., Abhilash, K. R., Geevarghese, G. A., Muruganandam, R., Gopi, M., Raja, S., Das, R. R., Patro, S., Krishnan, P., & Ramesh, R. (2020). Salt marsh vegetation in India: Species composition, distribution, zonation pattern and conservation implications. *Estuarine, Coastal and Shelf Science*, *242*, 106792.

Wright, M. N., & Ziegler, A. (2017). Ranger: A fast implementation of random forests for high dimensional data in C++ and R. *Journal of Statistical Software*, *77*(1), 1–17.

Yamazaki, D., Ikeshima, D., Tawatari, R., Yamaguchi, T., O'Loughlin, F., Neal, J. C., Sampson, C. C., Kanae, S., & Bates, P. D. (2017). A high-accuracy map of global terrain elevations. *Geophysical Research Letters*, *44*(11), 5844–5853.

Zhang, X., Liu, L., Zhao, T., Chen, X., Lin, S., Wang, J., Mi, J., & Liu, W. (2023). GWL_FCS30: A global 30 m wetland map with a fine classification system using multi-sourced and time-series remote sensing imagery in 2020. *Earth System Science Data*, *15*(1), 265–293.

Zheng, S., Shao, D., & Sun, T. (2018). Productivity of invasive saltmarsh plant *Spartina alterniflora* along the coast of China: A meta-analysis. *Ecological Engineering*, *117*, 104–110.

zu Ermgassen, P. S. E., Baker, R., Beck, M. W., Dodds, K., zu Ermgassen, S. O. S. E., Mallick, D., Taylor, M. D., & Turner, R. E. (2021). Ecosystem services: Delivering decision-making for salt marshes. *Estuaries and Coasts*, *44*(6), 1691–1698.

BIOSKETCH

The Global Coastal Wetlands Lab's focus is to provide research with furthers biodiversity conservation and restoration of coastal wetlands, including quantifying their value to people. The research is predominately data-driven analyses at landscape and global scales.

SUPPORTING INFORMATION

Additional supporting information can be found online in the Supporting Information section at the end of this article.